Figure S1

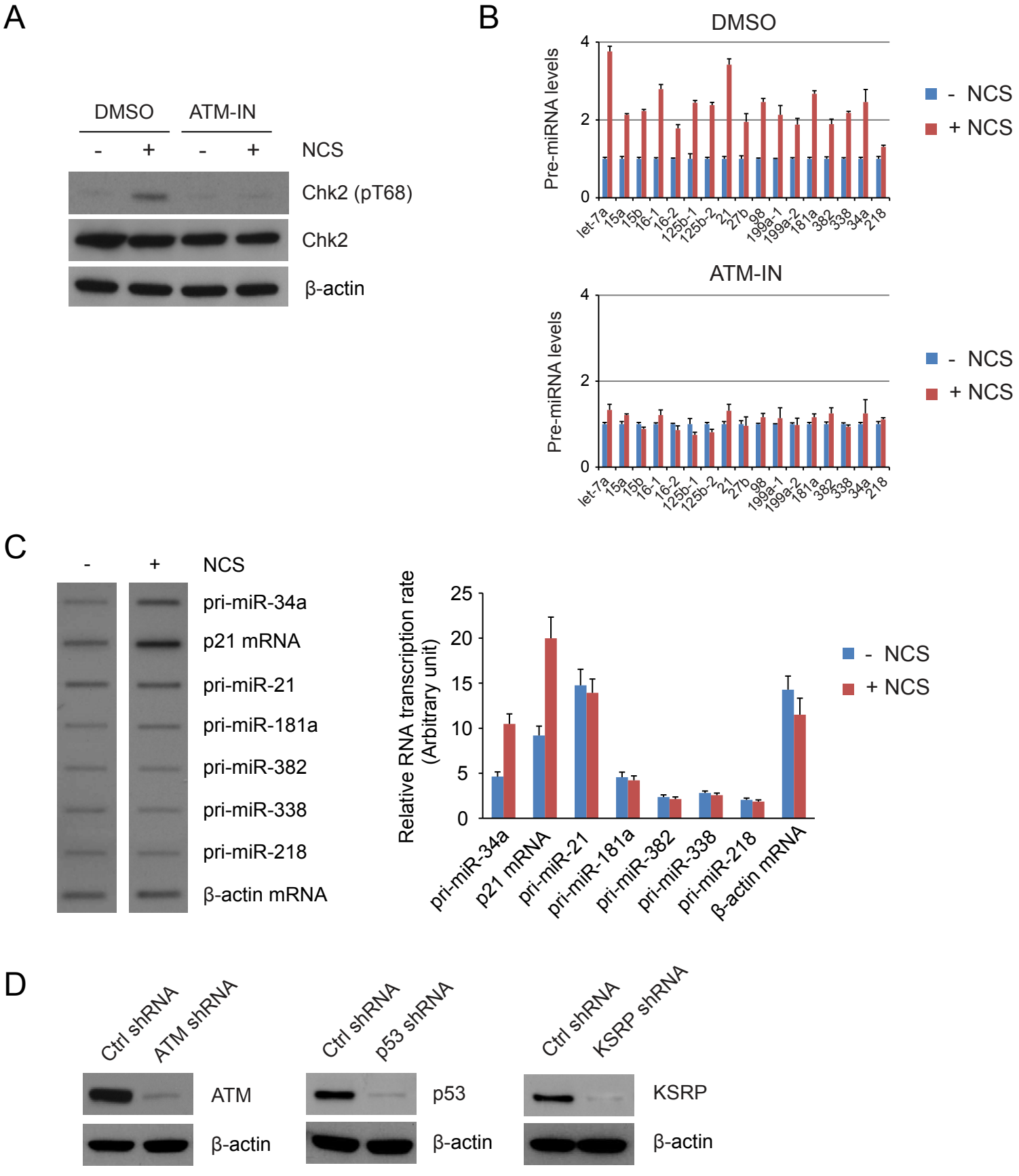
A
DMSO
ATM-IN
- + - +
NCS
Chk2 (pT68)
Chk2
β-actin
B
DMSO
Pre-miRNA levels
- NCS
+ NCS
let-7a 15a 15b 16-1 16-2 125b-1 125b-2 21 27b 98 199a-1 199a-2 181a 382 338 34a 218
ATM-IN
C
- + NCS
pri-miR-34a
p21 mRNA
pri-miR-21
pri-miR-181a
pri-miR-382
pri-miR-338
pri-miR-218
β-actin mRNA
Relative RNA transcription rate (Arbitrary unit)
D
Ctrl shRNA
ATM shRNA
p53 shRNA
KSRP shRNA
ATM
p53
KSRP
β-actin

Figure S2

A

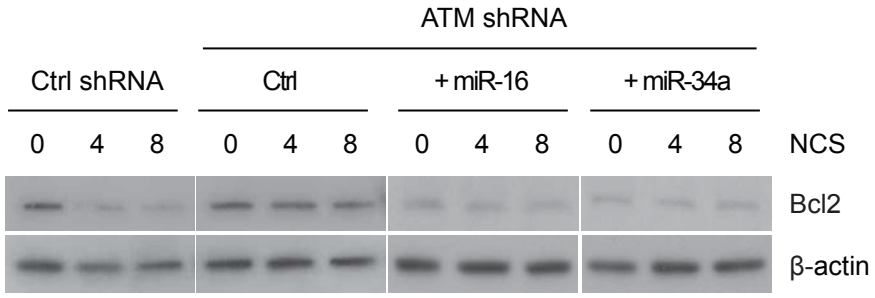

B

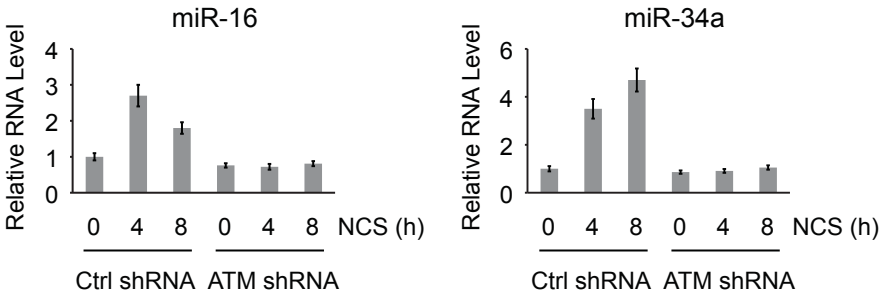

C

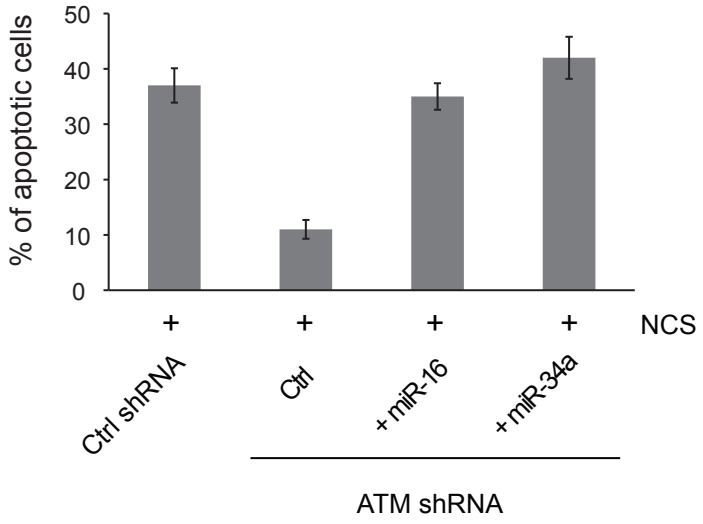

Figure S3

A

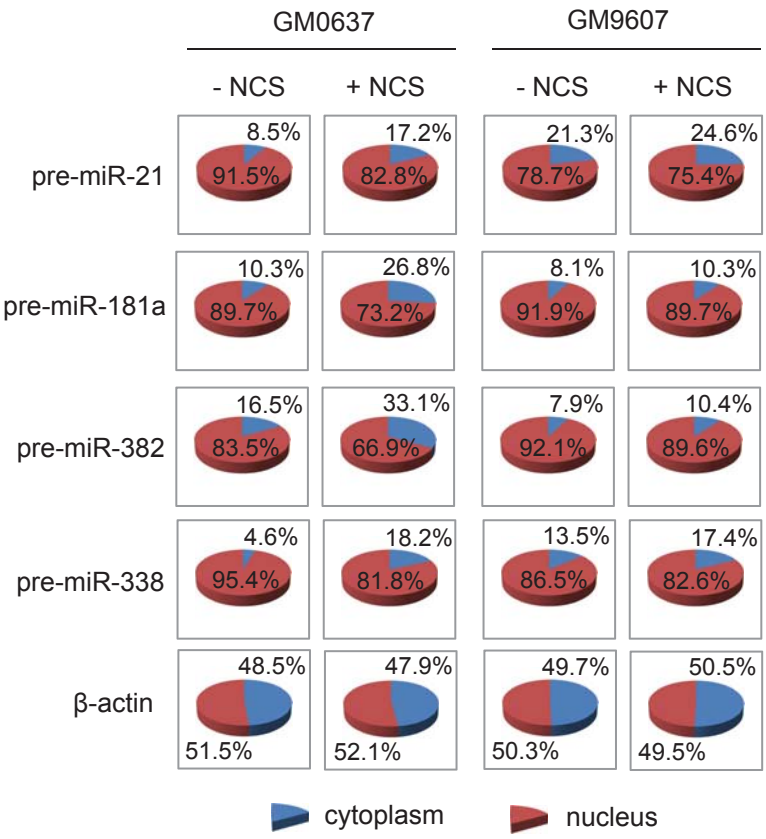
GM0637
GM9607
- NCS
+ NCS
- NCS
+ NCS
pre-miR-21
8.5%
91.5%
17.2%
82.8%
21.3%
78.7%
24.6%
75.4%
pre-miR-181a
10.3%
89.7%
26.8%
73.2%
8.1%
91.9%
10.3%
89.7%
pre-miR-382
16.5%
83.5%
33.1%
66.9%
7.9%
92.1%
10.4%
89.6%
pre-miR-338
4.6%
95.4%
18.2%
81.8%
13.5%
86.5%
17.4%
82.6%
β-actin
48.5%
51.5%
47.9%
52.1%
49.7%
50.3%
50.5%
49.5%
cytoplasm
nucleus

B

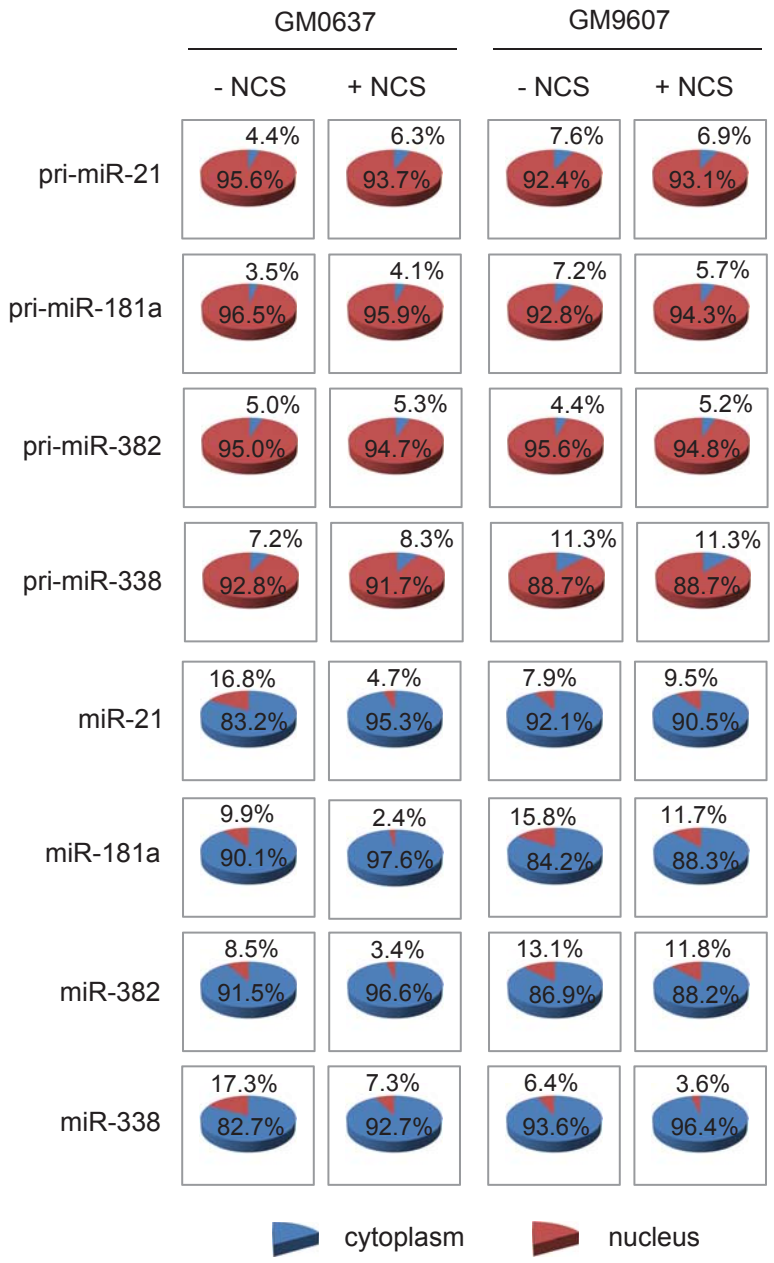
GM0637
GM9607
- NCS
+ NCS
- NCS
+ NCS
pri-miR-21
4.4%
95.6%
6.3%
93.7%
7.6%
92.4%
6.9%
93.1%
pri-miR-181a
3.5%
96.5%
4.1%
95.9%
7.2%
92.8%
5.7%
94.3%
pri-miR-382
5.0%
95.0%
5.3%
94.7%
4.4%
95.6%
5.2%
94.8%
pri-miR-338
7.2%
92.8%
8.3%
91.7%
11.3%
88.7%
11.3%
88.7%
miR-21
16.8%
83.2%
4.7%
95.3%
7.9%
92.1%
9.5%
90.5%
miR-181a
9.9%
90.1%
2.4%
97.6%
15.8%
84.2%
11.7%
88.3%
miR-382
8.5%
91.5%
3.4%
96.6%
13.1%
86.9%
11.8%
88.2%
miR-338
17.3%
82.7%
7.3%
92.7%
6.4%
93.6%
3.6%
96.4%
cytoplasm
nucleus

Figure S4

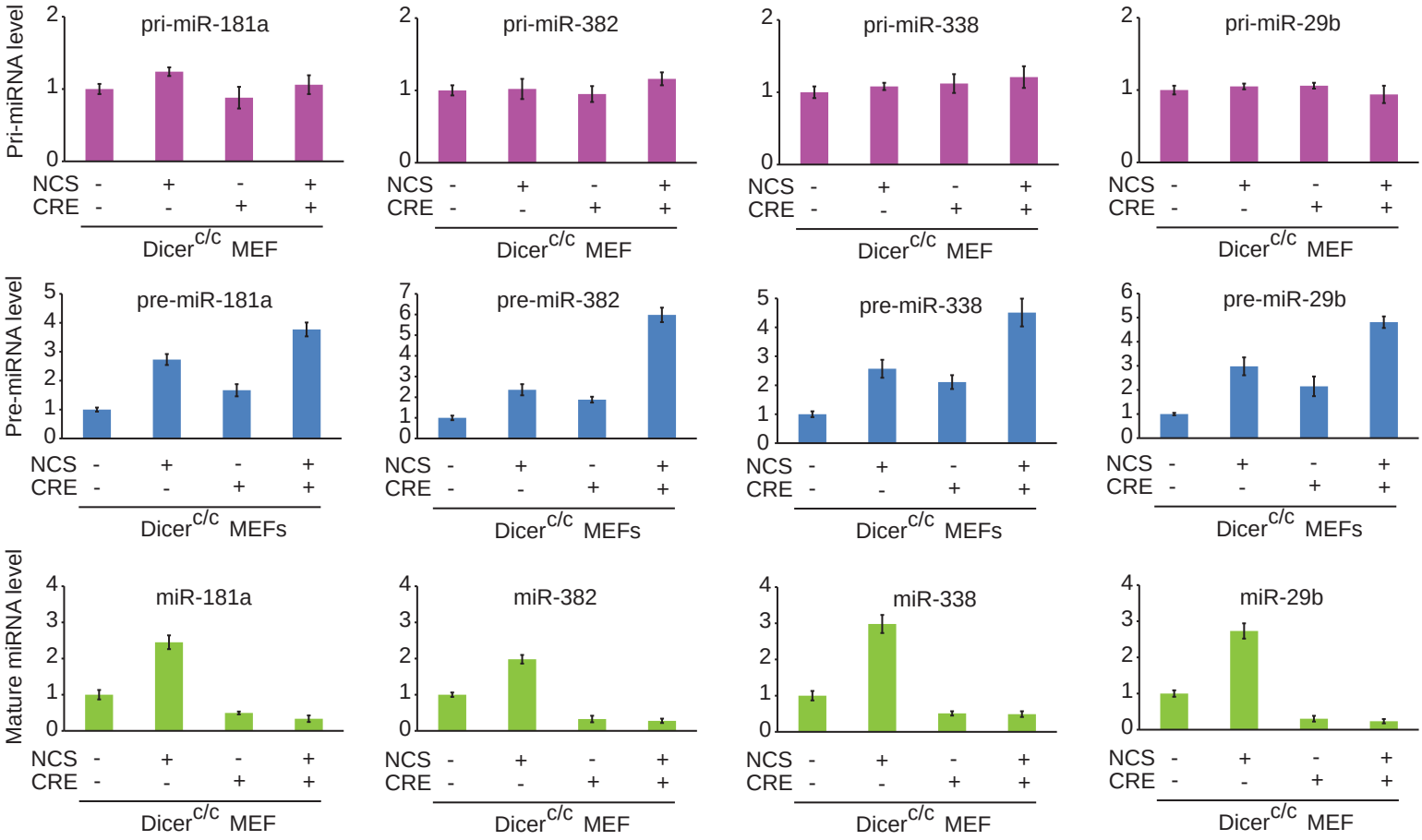
Pri-miRNA level
pri-miR-181a
pri-miR-382
pri-miR-338
pri-miR-29b
Pre-miRNA level
pre-miR-181a
pre-miR-382
pre-miR-338
pre-miR-29b
Mature miRNA level
miR-181a
miR-382
miR-338
miR-29b
NCS
CRE
Dicer c/c MEF
Dicer c/c MEFs

Figure S5

A

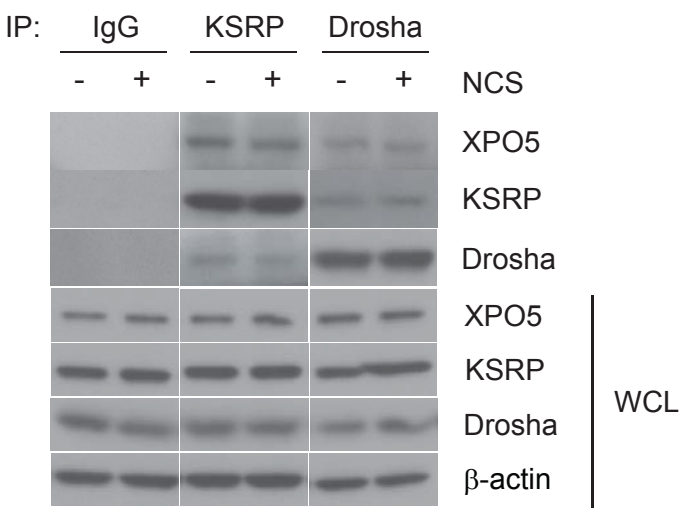
IP:
IgG
KSRP
Drosha
- + - + - +
NCS
XPO5
KSRP
Drosha
XPO5
KSRP
Drosha
β-actin
WCL

B

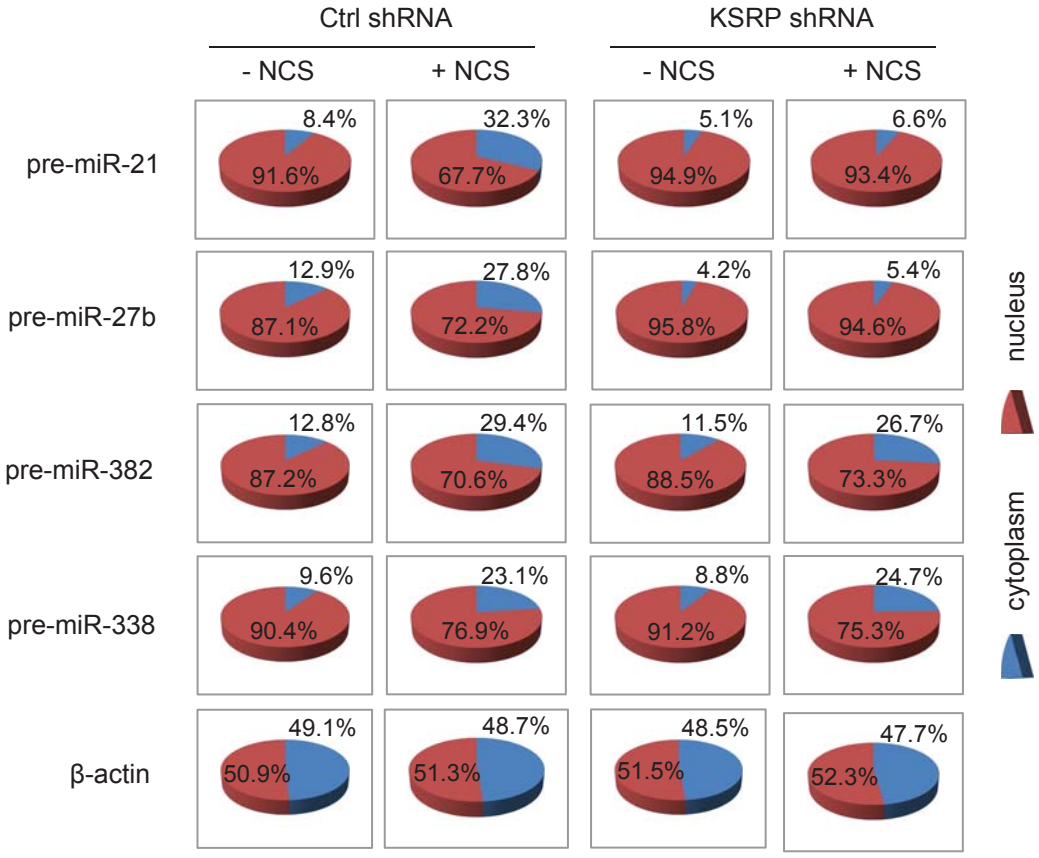
Ctrl shRNA
KSRP shRNA
- NCS
+ NCS
- NCS
+ NCS
pre-miR-21
8.4%
91.6%
32.3%
67.7%
5.1%
94.9%
6.6%
93.4%
pre-miR-27b
12.9%
87.1%
27.8%
72.2%
4.2%
95.8%
5.4%
94.6%
pre-miR-382
12.8%
87.2%
29.4%
70.6%
11.5%
88.5%
26.7%
73.3%
pre-miR-338
9.6%
90.4%
23.1%
76.9%
8.8%
91.2%
24.7%
75.3%
β-actin
49.1%
50.9%
48.7%
51.3%
48.5%
51.5%
47.7%
52.3%
nucleus
cytoplasm

Figure S6

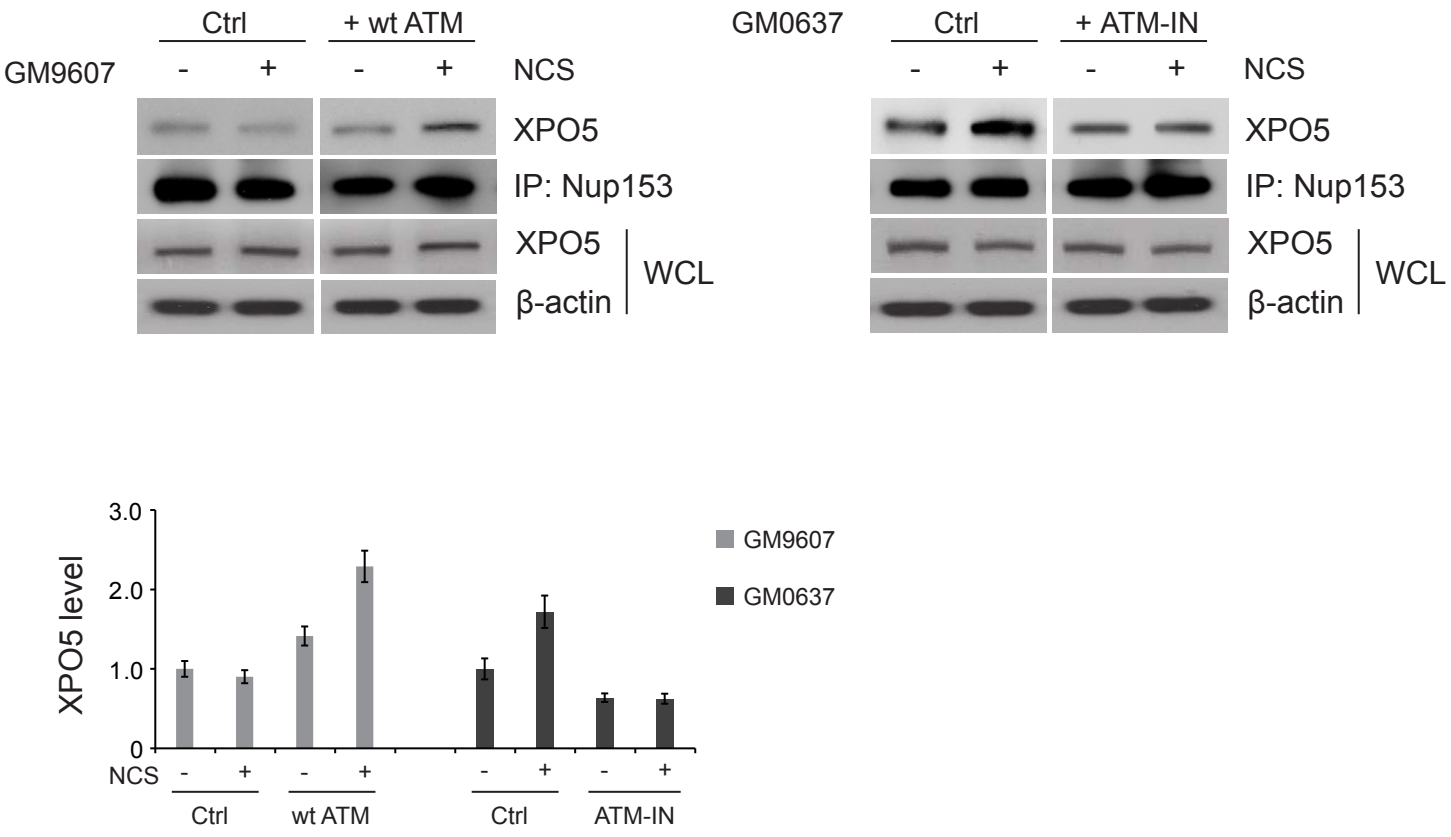
Ctrl
+ wt ATM
GM9607
- + - +
NCS
XPO5
IP: Nup153
XPO5
β-actin
WCL
GM0637
Ctrl
+ ATM-IN
- + - +
NCS
XPO5
IP: Nup153
XPO5
β-actin
WCL
3.0
2.0
1.0
0
XPO5 level
GM9607
GM0637
NCS - + - + - + - +
Ctrl
wt ATM
Ctrl
ATM-IN

Figure S7

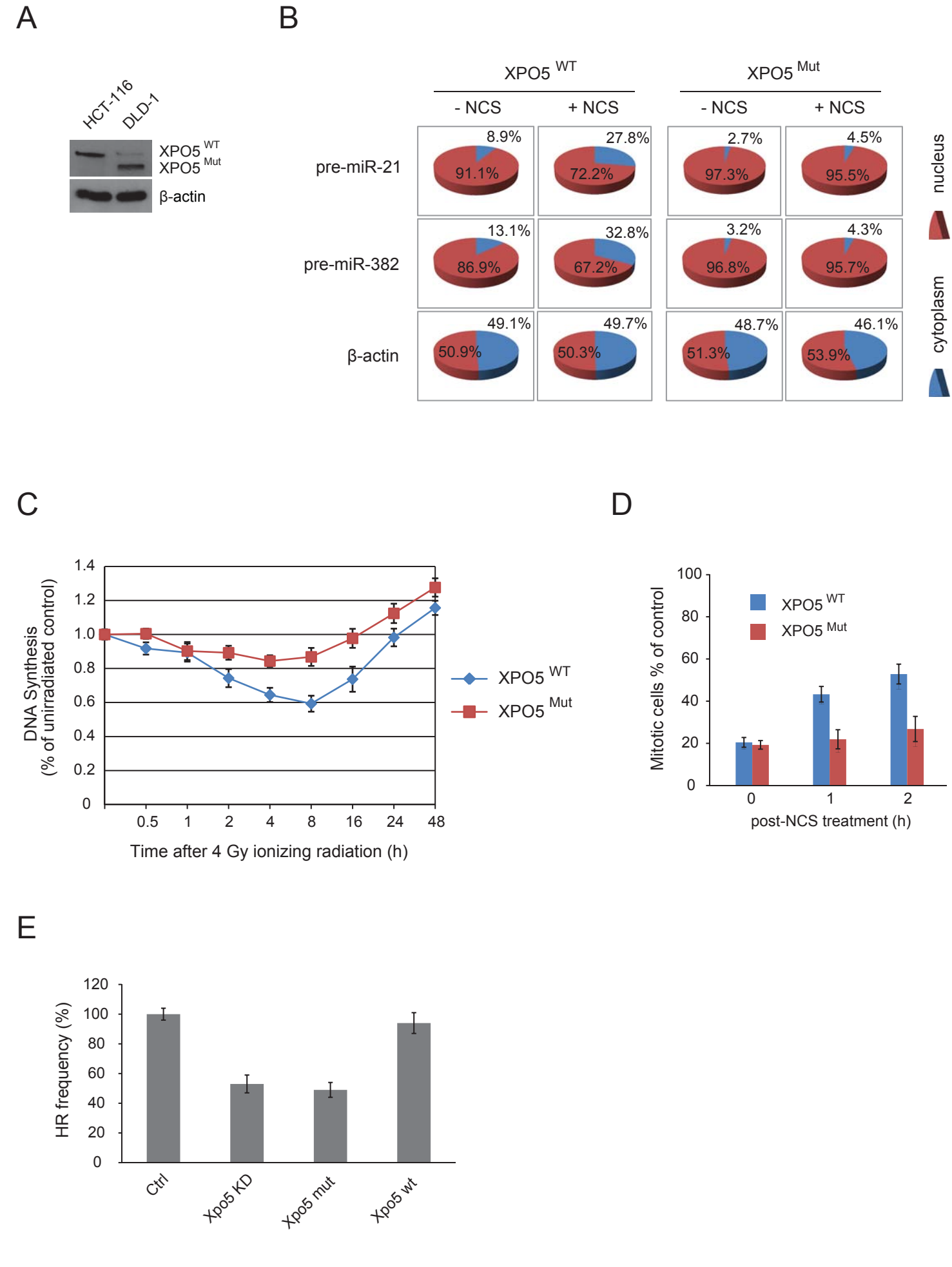
A
HCT-116
DLD-1
XPO5 WT
XPO5 Mut
β-actin
B
XPO5 WT
XPO5 Mut
- NCS
+ NCS
- NCS
+ NCS
pre-miR-21
8.9%
91.1%
27.8%
72.2%
2.7%
97.3%
4.5%
95.5%
pre-miR-382
13.1%
86.9%
32.8%
67.2%
3.2%
96.8%
4.3%
95.7%
β-actin
49.1%
50.9%
49.7%
50.3%
48.7%
51.3%
46.1%
53.9%
nucleus
cytoplasm
C
DNA Synthesis (% of unirradiated control)
1.4
1.2
1.0
0.8
0.6
0.4
0.2
0
0.5
1
2
4
8
16
24
48
Time after 4 Gy ionizing radiation (h)
XPO5 WT
XPO5 Mut
D
Mitotic cells % of control
100
80
60
40
20
0
XPO5 WT
XPO5 Mut
0
1
2
post-NCS treatment (h)
E
HR frequency (%)
120
100
80
60
40
20
0
Ctrl
Xpo5 KD
Xpo5 mut
Xpo5 wt

Figure S8

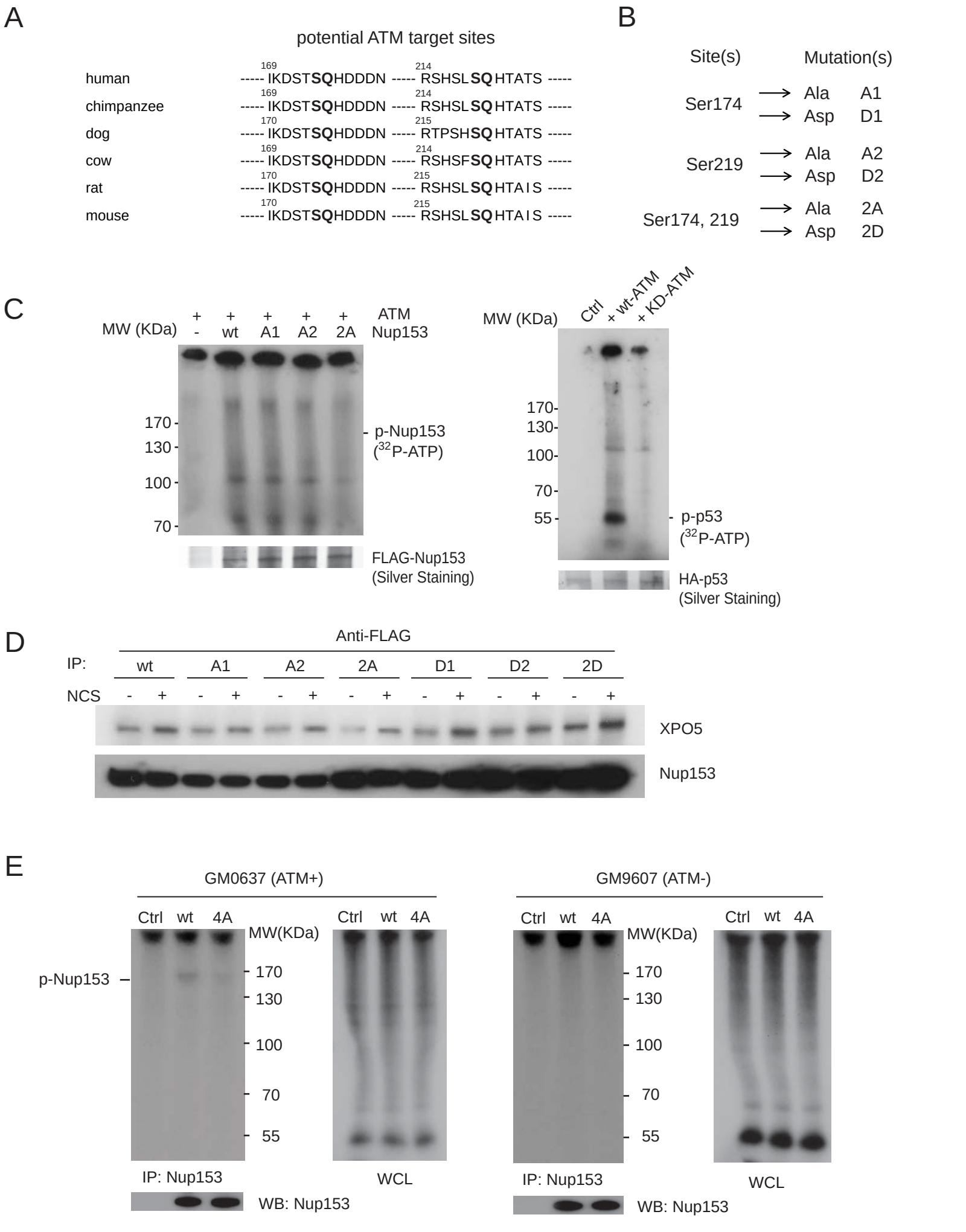
A
potential ATM target sites
human ----- IKDST**SQ**HDDDN ----- RSHSL**SQ**HTATS -----
chimpanzee ----- IKDST**SQ**HDDDN ----- RSHSL**SQ**HTATS -----
dog ----- IKDST**SQ**HDDDN ----- RTPSH**SQ**HTATS -----
cow ----- IKDST**SQ**HDDDN ----- RSHSF**SQ**HTATS -----
rat ----- IKDST**SQ**HDDDN ----- RSHSL**SQ**HTAIS -----
mouse ----- IKDST**SQ**HDDDN ----- RSHSL**SQ**HTAIS -----
B
Site(s)
Mutation(s)
Ser174 → Ala A1
→ Asp D1
Ser219 → Ala A2
→ Asp D2
Ser174, 219 → Ala 2A
→ Asp 2D
C
MW (KDa)
+ - + wt + A1 + A2 + 2A ATM Nup153
170
130
100
70
p-Nup153 (32P-ATP)
FLAG-Nup153 (Silver Staining)
MW (KDa)
Ctrl + wt-ATM + KD-ATM
170
130
100
70
55
p-p53 (32P-ATP)
HA-p53 (Silver Staining)
D
Anti-FLAG
IP: wt A1 A2 2A D1 D2 2D
NCS - + - + - + - + - + - + - +
XPO5
Nup153
E
GM0637 (ATM+)
Ctrl wt 4A
MW(KDa)
p-Nup153
170
130
100
70
55
IP: Nup153
WB: Nup153
Ctrl wt 4A
WCL
GM9607 (ATM-)
Ctrl wt 4A
MW(KDa)
170
130
100
70
55
IP: Nup153
WB: Nup153
Ctrl wt 4A
WCL

Figure S9

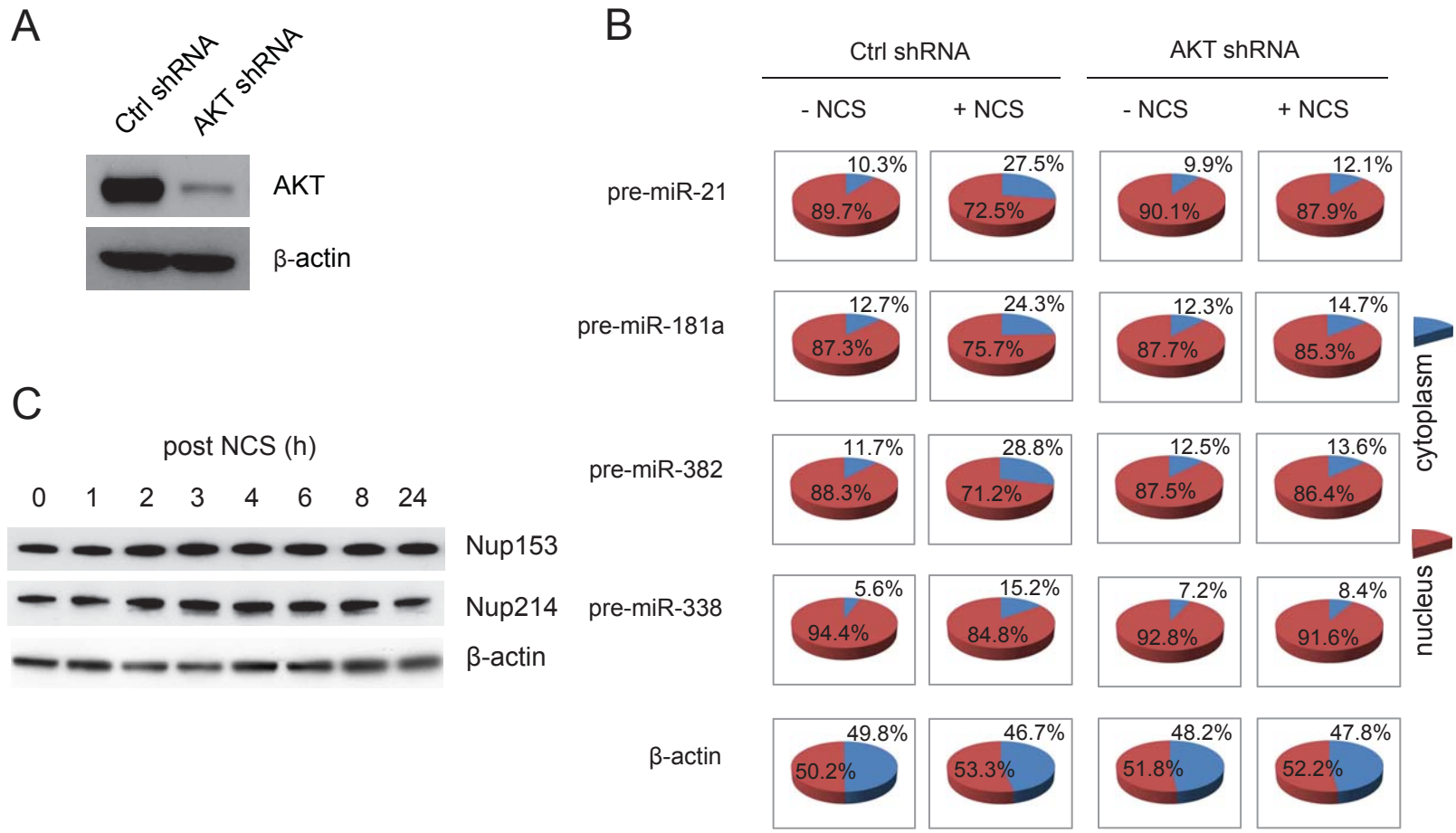
A
Ctrl shRNA
AKT shRNA
AKT
β-actin
B
Ctrl shRNA
AKT shRNA
- NCS
+ NCS
- NCS
+ NCS
pre-miR-21
10.3%
89.7%
27.5%
72.5%
9.9%
90.1%
12.1%
87.9%
pre-miR-181a
12.7%
87.3%
24.3%
75.7%
12.3%
87.7%
14.7%
85.3%
pre-miR-382
11.7%
88.3%
28.8%
71.2%
12.5%
87.5%
13.6%
86.4%
pre-miR-338
5.6%
94.4%
15.2%
84.8%
7.2%
92.8%
8.4%
91.6%
β-actin
49.8%
50.2%
46.7%
53.3%
48.2%
51.8%
47.8%
52.2%
cytoplasm
nucleus
C
post NCS (h)
0 1 2 3 4 6 8 24
Nup153
Nup214
β-actin

Figure S10

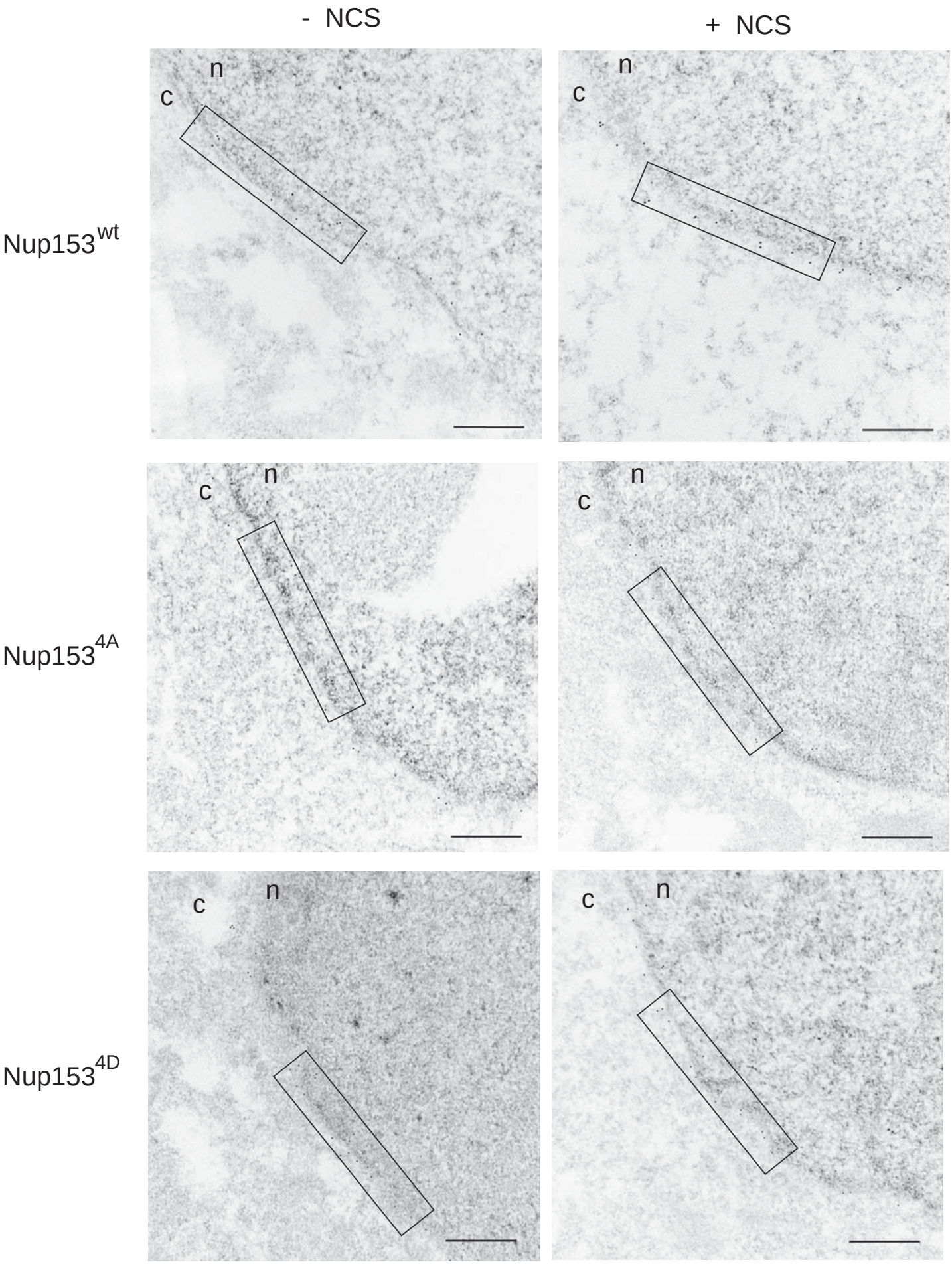

Figure S11

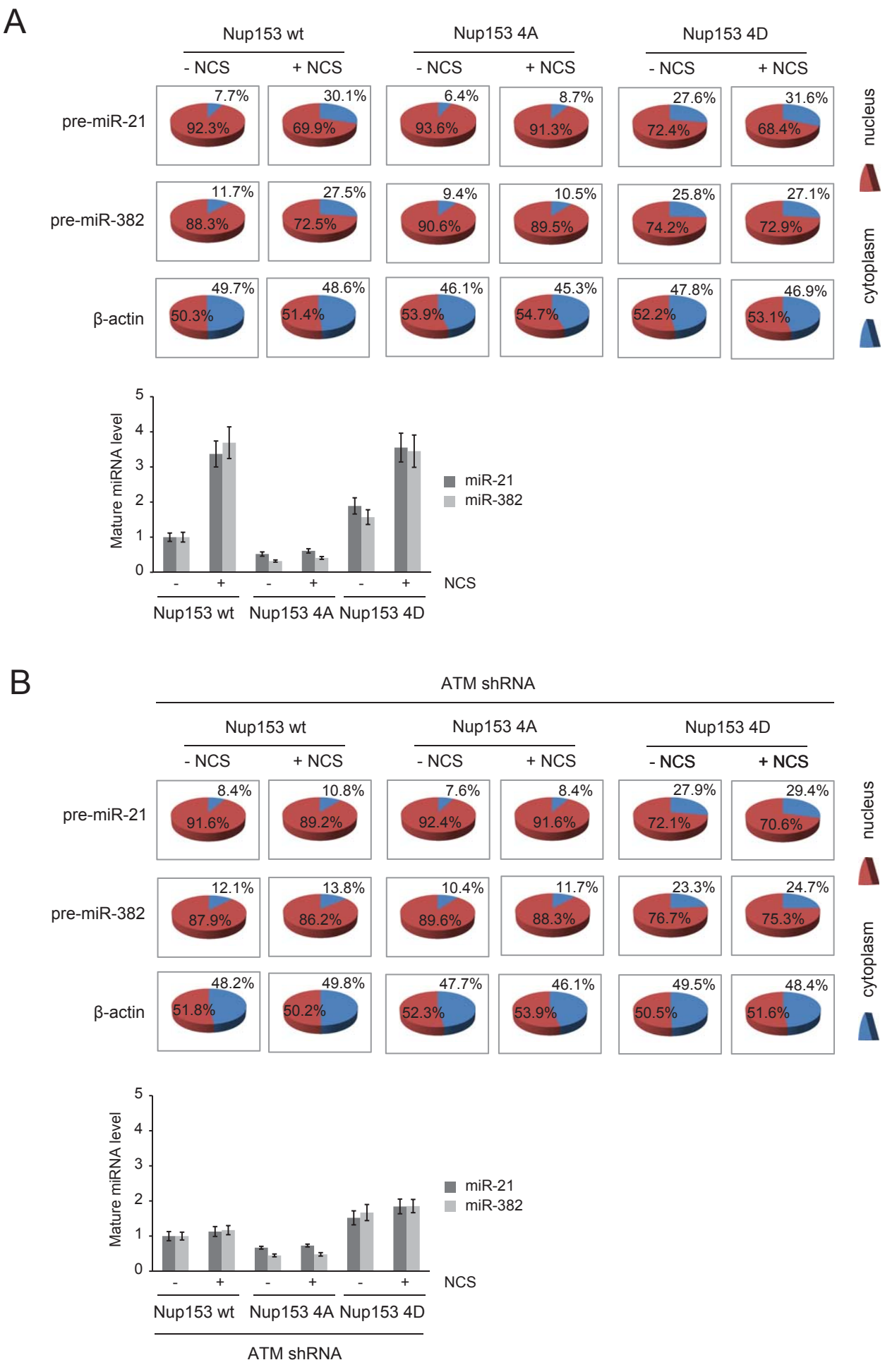
A
Nup153 wt
Nup153 4A
Nup153 4D
- NCS
+ NCS
pre-miR-21
pre-miR-382
β-actin
7.7%
92.3%
30.1%
69.9%
6.4%
93.6%
8.7%
91.3%
27.6%
72.4%
31.6%
68.4%
11.7%
88.3%
27.5%
72.5%
9.4%
90.6%
10.5%
89.5%
25.8%
74.2%
27.1%
72.9%
49.7%
50.3%
48.6%
51.4%
46.1%
53.9%
45.3%
54.7%
47.8%
52.2%
46.9%
53.1%
nucleus
cytoplasm
Mature miRNA level
miR-21
miR-382
NCS
B
ATM shRNA
8.4%
91.6%
10.8%
89.2%
7.6%
92.4%
8.4%
91.6%
27.9%
72.1%
29.4%
70.6%
12.1%
87.9%
13.8%
86.2%
10.4%
89.6%
11.7%
88.3%
23.3%
76.7%
24.7%
75.3%
48.2%
51.8%
49.8%
50.2%
47.7%
52.3%
46.1%
53.9%
49.5%
50.5%
48.4%
51.6%

Figure S12

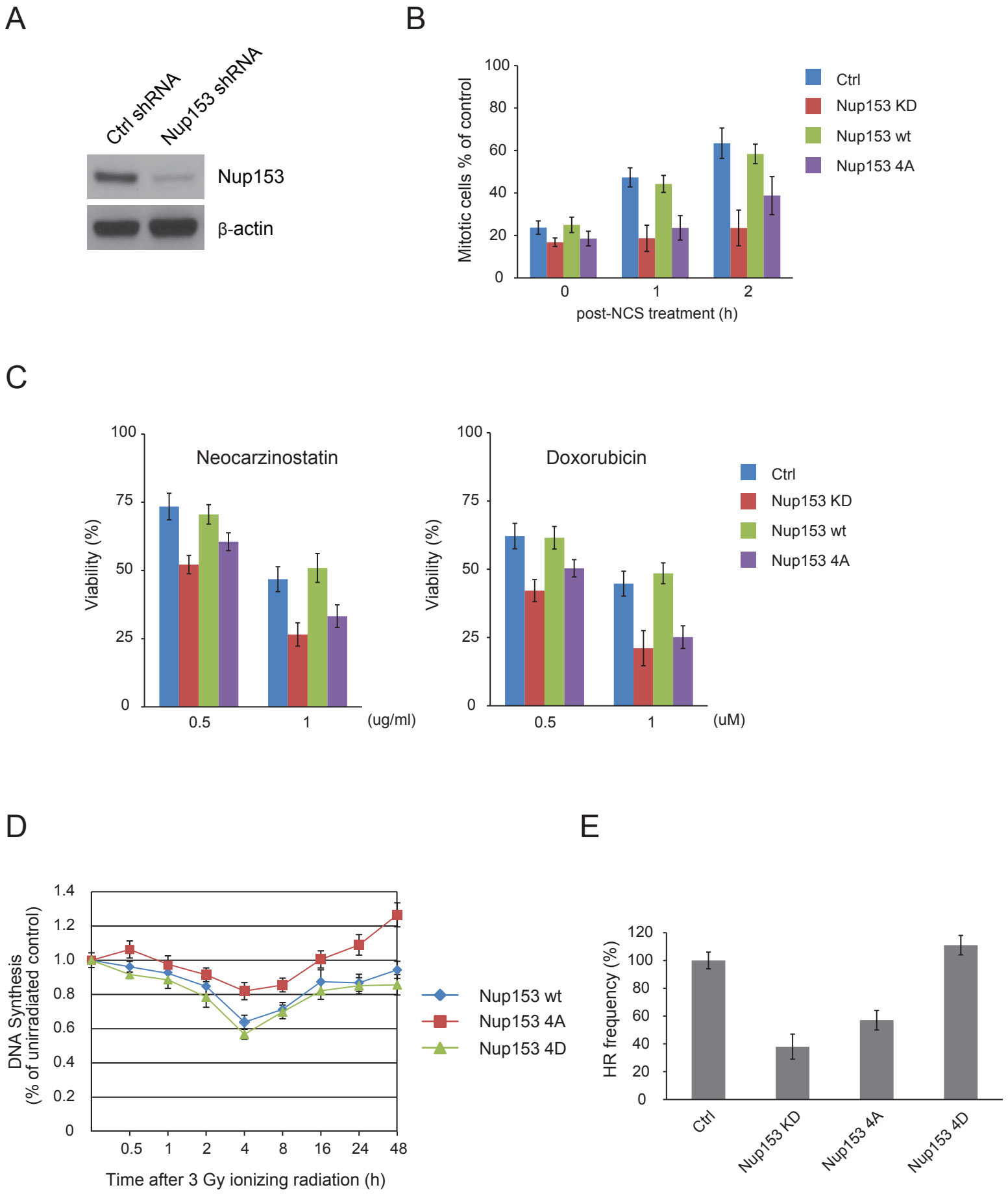
A
Ctrl shRNA
Nup153 shRNA
Nup153
β-actin
B
Mitotic cells % of control
100
80
60
40
20
0
0
1
2
post-NCS treatment (h)
Ctrl
Nup153 KD
Nup153 wt
Nup153 4A
C
Neocarzinostatin
Viability (%)
100
75
50
25
0
0.5
1
(ug/ml)
Doxorubicin
Viability (%)
100
75
50
25
0
0.5
1
(uM)
Ctrl
Nup153 KD
Nup153 wt
Nup153 4A
D
DNA Synthesis
(% of unirradiated control)
1.4
1.2
1.0
0.8
0.6
0.4
0.2
0
0.5
1
2
4
8
16
24
48
Time after 3 Gy ionizing radiation (h)
Nup153 wt
Nup153 4A
Nup153 4D
E
HR frequency (%)
120
100
80
60
40
20
0
Ctrl
Nup153 KD
Nup153 4A
Nup153 4D

SUPPLEMENTAL FIGURE LEGENDS

Figure S1 (related to Figure 1). ATM-dependent posttranscriptional regulation of miRNA expression. (**A**) ATM inhibitor KU55933 inhibits ATM activity in GM0637 cells. ATM activity is indicated by the T68 phosphorylation of Chk2. (**B**) DNA damage induces pre-miRNA levels in an ATM-dependent manner. GM0637 cells were treated as in Figure 1A. Error bars represents the mean ± SD. (**C**) Transcription of miRNA genes are not induced after DNA damage. Run-on assays were performed to measure the transcription activity of the indicated miRNA genes in GM0637 cells treated with or without NCS. Radioactivity of each band was quantified by a liquid scintillation counter. (**D**) ATM, p53 and KSRP are knocked down by their specific shRNAs.

Figure S2 (related to Figure 1). DNA damage-induced miRNAs regulate apoptosis in the DDR. (A) Suppression of Bcl2 after DNA damage is abolished by ATM knockdown, but restored by ectopic expression of miR-16 or miR-34a. **(B)** miR-16 and miR-34a are induced in an ATM-dependent manner after DNA damage. **(C)** Ectopic expression of miR-16 or miR-34a restored cell apoptosis after DNA damage.

Figure S3 (related to Figure 2). Distribution of pri-miRNAs, pre-miRNAs and mature miRNAs in the nucleus and cytoplasm after DNA damage. (**A**) Cytoplasmic distribution of pre-miRNAs is increased after DNA damage in GM0637 cells, but not in GM9607 cells. Levels of 4 pre-miRNAs were examined by quantitative RT-PCR. (**B**) DNA damage has no significant effect on the intracellular distribution of pri-miRNAs and miRNAs. Levels of 4 pri-miRNAs and their corresponding mature miRNAs in the nucleus and cytoplasm are examined by quantitative RT-PCR in the cells described above. Error bars represent the mean ± SD.

Figure S4 (related to Figure 2). Posttranscriptional induction of miRNAs in mouse embryonic fibroblasts. Precursor and mature forms of four representative miRNAs are induced after DNA damage in control Dicer$^{c/c}$ MEFs, but not in Dicer$^{c/c}$ MEFs expressing adenoviral Cre recombinase. Primary transcripts of these miRNAs are unchanged after DNA damage. Error bars represent the mean ± SD.

Figure S5 (related to Figure 3). Increased Drosha-mediated processing is a prerequisite for the induced nuclear export of pre-miRNAs. (A) XPO5 and KSRP are in the Drosha complex. **(B)** Knockdown of KSRP inhibited nuclear export of KSRP-dependent pre-miR-21 and pre-miR-27b, but not other DNA damage-induced pre-miRNAs (pre-miR-382 and pre-miR-338).

Figure S6 (related to Figure 4). DNA damage induces Nup153-XPO5 interaction in an ATM-dependent manner. GM0637 and GM9607 cells were treated with or without NCS. Protein interactions were examined by immunoprecipitation-Western blot. Activity of ATM was manipulated by overexpression in GM9607 cells or by ATM inhibitor in GM0637 cells. Band intensities were measured by phosphoimager and error bars represent the mean ± SD.

Figure S7 (related to Figure 4). Functionally deficient mutant XPO5 fails to act in pre-miRNA nuclear export in the DDR. (A) Wildtype and mutant XPO5 are expressed in HCT116 and DLD-1 cells, respectively. **(B)** Nuclear export of pre-miRNAs is induced after DNA damage in the wildtype XPO5-reintroduced DLD-1 cells, but not in control DLD-1 cells expressing mutant XPO5. **(C)** Expression of wildtype XPO5 restored intra-S cell cycle checkpoint activity

after DNA damage. **(D)** Expression of wildtype XPO5 restored G2/M cell cycle checkpoint activity after DNA damage. **(E)** Knockdown of XPO5 inhibits homologous recombination DNA repair activity, which is rescued by ectopic expression of shRNA-resistant wildtype XPO5, but not mutant XPO5.

Figure S8 (related to Figure 5). Nup153 is not directly phosphorylated by ATM. (**A**) Putative ATM phosphorylated sites on Nup153. (**B**) Point mutations were generated on the putative phosphorylation sites. (**C**) Nup153 is not phosphorylated by ATM. Immunopurified wildtype or mutant Nup153 was incubated with immunopurified ATM kinase in a kinase reaction buffer containing ^{32}P-ATP. The phosphorylated proteins were run on SDS-PAGE and visualized by radiography (left panel). Immunoprecipitated Nup153 proteins were analyzed by silver staining. Purified HA-p53 was used as a positive control for the kinase activity of ATM (right panel). (**D**) Mutating putative ATM phosphorylation sites on Nup153 has no effect on the XPO5-Nup153 interaction. HCT116 cells overexpressing wildtype and mutant Nup153 were treated with NCS and immunoprecipitated with anti-FLAG antibody. XPO5 in the Nup153 immunoprecipitates was detected by Western blotting. (**E**) Nup153 is phosphorylated in vivo in an ATM-dependent manner. GM0637 and GM9607 cells were transfected with control vector or vector expressing FLAG-tagged wildtype or mutant form of Nup153. Cells were labeled with ^{32}P-orthophate 24 h after transfection, and Nup153 protein was immunoprecipitated and analyzed by SDS-PAGE and Western blotting. WCL: whole cell lysate.

Figure S9 (related to Figure 6). AKT promotes pre-miRNA nuclear export after DNA damage. (**A**) AKT is knocked down by its shRNA in HCT116 cells. (**B**) DNA damage-induced

nuclear export of pre-miRNAs is dependent on AKT. Levels of pre-miRNAs were measured by quantitative RT-PCR in control or AKT-knockdown HCT116 cells treated with or without NCS. (**C**) Protein levels of Nup153 and Nup214 are unchanged in the DNA damage response. HCT116 cells were treated with NCS and harvested at the indicated time points.

Figure S10 (related to Figure 7). AKT phosphorylation induces Nup153 structural change on the nuclear membrane. These images are original immune-EM images from which partial magnified images in Figure 7A were obtained.

Figure S11 (related to Figure 7). Phosphorylation-mutant Nup153 is defective in pre-miRNA nuclear export after DNA damage. Ectopic expression of shRNA-resistant wildtype Nup153, but not mutant Nup153, restores the DNA damage induction of pre-miRNA nuclear export in HCT116 cells with endogenous Nup153 knockdown in the presence of ATM **(A)**, but not when ATM is knocked down **(B)**.

Figure S12 (related to Figure 7). AKT phosphorylation contributes to the biological functions of Nup153 in the DDR. (**A**) Nup153 is knocked down by its specific shRNA. (**B**) Knockdown of Nup153 reduces mitotic activity, which is rescued by ectopic expression of shRNA-resistant wildtype or 4D mutant Nup153, but not phospho-deficient 4A mutant Nup153. (**C**) Knockdown of Nup153 sensitizes cells to DNA damage stress. Expression of wildtype or 4D mutant Nup153, but not 4A mutant Nup153, decreased the sensitivity of the Nup153 knockdown cells to DNA damage stress. The Nup153 knockdown HCT116 cells were transfected with control vector or vectors expressing shRNA-resistant wildtype or mutant Nup153. The cells were

treated with NCS or doxorubicin at indicated concentrations and cell viability was measured two days after treatment. **(D)** HCT116 cells expressing 4A mutant Nup153 have weaker intra-S cell cycle checkpoint as indicated by S-phase DNA synthesis. **(E)** Knockdown of Nup153 inhibits homologous recombination, which is rescued by ectopic expression of shRNA-resistant 4D mutant Nup153, but not 4A mutant Nup153.

SUPPLEMENTAL EXPERIMENTAL PROCEDURES

Western Blot Analysis, Antibodies, and Purified Proteins

Immunoprecipitations, Western blot analysis, and immunoprecipitation-Western blot analyses were performed by standard methods described previously (Lu et al., 2005). To dissociate proteins from nuclear membrane, 0.5% sodium deoxycholate and 0.1% Brij35 were added into lysis buffer. Anti-actin (#1616), anti-p53 (#126), anti-Lamin B (#6216), anti-α tublin (#12462), HRP-anti-goat IgG (#2020), HRP-anti-rabbit IgG (#2054), and HRP-anti-mouse IgG (#2055) antibodies were purchased from Santa Cruz; Anti-Dicer (#ab14601), anti-Expotin-5 (#ab57491) and anti-Ran (ab4781) antibodies were purchased from Abcam; Anti-phospho-p53,Ser15 (#9286), anti-phospho-Akt, Ser473 (#9271), anti-Akt (#9272), anti-phospho-GSK-3α/β, Ser21/9 (#9327), anti-GSK-3α/β (#5676) antibodies were purchased from Cell Signaling. Anti-Nup153 (#NB100-93329) antibody was purchased from Novus Biologicals. Anti-Nup214 (#A300-716A), anti-Drosha (#A301-886A) antibodies were purchased from Bethyl Laboratories. Gold particle-conjugated anti-mouse IgG (#EM.GMHL10) antibody was purchased from British Biocell. Purified recombinant protein of AKT (#TP301850) was purchased from Origene Technologies. GSK-3 fusion protein (#9237) was purchased from Cell Signaling.

Plasmid Constructs and Cell Transfection

The ATM expression vector was kindly provided by Dr. Michael Kastan at St Jude Children's Hospital. The Exportin-5 (wild type and mutant) expression constructs were generously provided by Dr. Manel Esteller at Bellvitge Biomedical Research Institute, Spain. The Nup214 expression vector was kindly provided by Dr. Toshimi Michigami at Osaka Medical Center for Maternal and Child Health, Japan. The Nup153 expression vector (#RC208264) was purchased from Origene. Using this construct, mutagenesis was performed by using QuikChange II XL Site-

Directed Mutagenesis Kit (#200521, Stratagene) to obtain constructs encoding mutant forms of Nup153, including mutations on the predicted ATM-phosphorylation sites, A1(S174A), A2(S219A), 2A(S174A, S219A), D1(S174D), D2(S219D), 2D(S174D, S219D), and predicted AKT-phosphorylation sites, 4A(S330A, S333A, S334A, S338A) and 4D(S330D, S333D, S334D, S338D). Lentiviral shRNA expression vectors for p53, ATM, KSRP and Nup153 knockdown were provided by ShRNA and ORFeome Core at the M.D. Anderson Cancer Center.

Nuclear Run-On Assay

The nuclear run-on assay was performed as described previously (Smale, 2009). An aliquot (1μg) of single-stranded DNA fragment (complementary to each specific miRNA transcript) was amplified by PCR as described by Tang X et al. (Tang et al., 2006) . DNA was plot-blotted onto 0.45 μm nitrocellulose membrane (Bio-rad). After isolation of the nucleus and run-on transcription reaction, RNA was isolated with Trizol reagent. Membranes were probed with ^{32}P-labelled run-on RNA, exposed to film and analyzed for intensity with a scintillation counter.

TUNEL Assay and Cell Viability Assay

TdT-mediated dUTP Nick End Labeling (TUNEL) assay was performed using the Click-iT TUNEL Alexa Fluor 594 Imaging Assay kit (#C10246, Invitrogen) according to manufacturer's instructions. Briefly, cells were grown on Millicell EZ slides (Millipore) and treated with NCS. At indicated time points, cells were fixed with 4% paraformaldehyde, subjected to TUNEL assay and counterstained with DAPI. The cells were visualized with Zeiss AxioVision fluorescent microscope. In cell viability assays, cells were seeded into 96-well plates at 3000 cells/well and incubated for 24 h. Each DNA damaging drug was then added at various concentrations to quadruplicate wells in a final volume of 100 μl of medium. After 24 h of incubation, cells were

cultured for 2 days and cell viability was measured using WST-1 reagent (Roche) following the manufacturer's instruction.

Nuclear and Cytoplasmic Proteins and Nuclear Envelope Extraction

Nuclear and cytoplasmic proteins were extracted using the NE-PER Nuclear and Cytoplasmic Extraction kit (#78833, Thermo Scientific). Extraction was carried out according to the manufacturer's instructions. For isolation of nuclear envelope, purified nuclei were resuspended in ice-cold 10% SHM buffer (0.3 M sucrose, 10 mM Hepes pH 7.4, 2 mM $MgCl_2$, 0.5 mM $CaCl_2$, 2 mM DTT and 1 X protease inhibitor), and incubated with DNase I (10 U/ml) and RNase A (1.4 μg/ml) on ice for 20 min. For a second digestion of chromatin, the pellet nuclei were incubated in ice-cold 10% SHM buffer with DNase I (50 U/ml) and RNase A (5 μg/ml) on ice for 20 min, subsequently washed with 10% SHM buffer containing 300 mM NaCl. The nuclei were transferred and underlaid with 0.15 volume of 30% SHKM buffer (0.9 M sucrose, 10 mM Hepes pH 7.4, 25 mM KCl, 2.5 mM $MgCl_2$, 2 mM DTT and 1 x protease inhibitor) to float digested chromatin away from the nuclear envelops. After the nuclei pellet was washed with 300 mM NaCl and ice-cold 10% SHM buffer containing 400 mM KCl, respectively, the purified nuclear envelopes were resuspended in ice-cold 10% SHM buffer and kept at -80°C.

***In vivo* and *in vitro* Phosphorylation Assays and AKT Kinase Activity Assay**

For *in vitro* phosphorylation assays, cell lysates were first immunoprecipitated with control anti-IgG antibody and protein A/G-agarose. Cleared supernatants were immunoprecipitated with anti-FLAG or anti-HA agarose, and the beads were washed with TGN buffer followed by TGN buffer containing 0.5 M LiCl, and two washes with kinase buffer (20 mM HEPES, pH7.5, 50 mM NaCl, 10 mM $MgCl_2$, 1 mM dithiothreitol, and 10 mM $MnCl_2$). The immunoprecipitate was

resuspended in 50 μl of kinase buffer containing 10 μCi of [γ-^{32}P] ATP and 1 μg of purified ATM or AKT at 30°C for 30 min and stopped by the addition of SDS-polyacrylamide gel electrophoresis loading buffer. The proteins were run in SDS-PAGE and dried for X-ray file exposure. For *in vivo* phosphorylation assays, cells were washed with phosphate-free DMEM (#11971-025, Invitrogen) and subsequently incubated with 0.5 mCi/ml of ^{32}P-orthophosphate in phosphate-free DMEM containing dialyzed FBS (#26400-036, Invitrogen) for 4 h at 37°C. Cells were lysed and cell lysates were immunoprecipitated by anti-FLAG antibodies. Nup153 immunoprecipitates were run in SDS-PAGE and then dried for X-ray file exposure.

AKT kinase activity assays were performed using a kit obtained from Cell Signaling (#9840) according to the manufacturer's instructions.

RNA Isolation, Quantitative RT-PCR and MiRNA Expression Microarray

Total RNA and small RNA were isolated by using *mir*Vana™ miRNA Isolation Kit (#AM1560, Ambion). Nuclear and cytoplasmic RNA were extracted using the Cytoplasmic and Nuclear RNA purification kit (#21000, Norgen). Extraction was carried out according to the manufacturer's instruction. Human miRNA microarray analysis was performed by Phalanx Biotech. Pri-miRNA transcripts were measured using TaqMan pri-miRNA assays and primers provided by Applied Biosystems. Mature miRNAs were measured by using SYBR Green Master Mix kits and primers obtained from Exiqon. SuperScript III Platinum SYBR Green One-Step qRT-PCR kit (#11745-100) was used to quantify precursor miRNAs by RT-qPCR. The pre-miRNA levels in the nucleus and cytoplasm were plotted as "mean percentage". The RT-PCR primers are shown in the following list.

List of RT-PCR primers

Name	Forward 5'-3'	Reverse 5'-3'
hsa-pre-miR-143	CTGTCTCCCAGCCTGAGGT	CAGACTCCCAACTGACCAGAG
hsa-pre-miR-181a	TGAGTTTTGAGGTTGCTTCAG	ATTCCAAACTCACCGACAGC
hsa-pre-miR-21	ATGTTGACTGTTGAATCTCATGG	TGTCAGACAGCCCATCGAC
hsa-pre-miR-218	GTGCTTGATCTAACCATGTGGT	GTGCTTGACGGAACCATGTT
hsa-pre-miR-338	TCTCCAACAATATCCTGGTGCTGA	CTTCAACAAAATCACTGATGCTGGA
hsa-pre-miR-382	TACTTGAAGAGAAGTTGTTCGTGGTGG	TACTGAAAAAAGTGTTGTCCGTGAATGA
hsa-β-actin	CTGGCACCCAGCACAATG	GGACAGCGAGGCCAGGAT
mmu-pre-miR-181a	GGTTGCTTCAGTGAACATT	ATAGGGTACAATCAACGGT
mmu-pre-miR-29b	GGAAGCTGGTTTCATATGGTG	AGAACACTGATTTCAAATGGTGC
mmu-pre-miR-382	TACTTGAAGAGAAGTTGTTCGTGG	TACTGAAAAAAGTGTTGTCCGTGA
mmu-Dicer	ACCCCAAAGCAATTCCAGAGT	TAACAAGGCTGGTCGGGTTT
mmu-β-actin	GGCACCACACCTTCTACAATG	GGGGTGTTGAAGGTCTCAAAC

Confocal Microscopy

HCT116 cells were grown on Millicell EZ slides (Millipore) and treated with NCS or DMSO alone for 4 h and then fixed in ice-cold acetone for 10 min. Samples were then washed with PBS, incubated with protein-blocking solution containing 5% normal horse serum and 1% normal goat serum in PBS for 20 min at room temperature, and then incubated with anti-Nup153 antibody for 18 h at 4°C. The samples were washed and then incubated with secondary Cy5 antibody

(Jackson ImmunoResearch Laboratories) for 1 h. All samples were rinsed and then briefly incubated with SYTOX green nucleic acid stain (Eugene). The slides were mounted with a glycerol/PBS solution containing 0.1 M propyl gallate (Sigma) to minimize fluorescent bleaching. Confocal images were collected on a Zeiss LSM 510 laser scanning microscope system (Carl Zeiss) equipped with a motorized Axioplan microscope, argon laser, HeNe laser, LSM 510 control and image acquisition software, and appropriate filters (Chroma Technology).

Homologous Recombination DNA Repair Analysis

DR-U2OS cell line containing a single copy of the homologous recombination (HR) repair reporter substrate DR-GFP in a random locus was generated and previously described (Wan et al., 2013). DR-U2OS cells were infected with lentiviruses (pLKO.1 puro, Addgene) expressing control, XPO5 shRNA or Nup153 shRNA. Cells were transfected with shRNA-resistant mutant or wildtype XPO5 vectors, or shRNA-resistant mutant Nup153 (4A or 4D) vectors, respectively. After incubated for 48 h, cells were transfected with control or I-SceI-expressing plasmid. Flow cytometric analysis was performed to detect GFP positive cells on Guava EasyCyte™ Flow Cytometer (Millipore, USA) and relative HR frequencies were calculated.

Cell Cycle Checkpoint Assays

The intra-S-phase checkpoint assay was performed as previously described (Lu et al., 2005). Briefly, cells were prelabeled with 10 nCi/ml of [^{14}C] thymidine (Perkin Elmer) for 24 h. Cells were irradiated and incubated for the time indicated and pulse-labeled with 2.5 μCi of [^{3}H] thymidine (Perkin Elmer) for 15 min. Cells were harvested at various time points after irradiation and fixed with 70% methanol. The account of radioactivity was assayed in a liquid scintillation counter. ^{3}H counts were normalized with ^{14}C counts. The G2/M-phase assay was assessed by

histone H3 phosphorylation according to the PathScan Phospho-Histone H3 (Ser10) Sandwich ELISA Kit (Cell Signaling Technology).

References

Lu, X., Nannenga, B., and Donehower, L.A. (2005). PPM1D dephosphorylates Chk1 and p53 and abrogates cell cycle checkpoints. Genes Dev 19, 1162-1174.

Smale,S.T. (2009). Nuclear run-on assay. Cold Spring Harb. Protoc. *2009*, db.

Tang,X., Morris,S.L., Langone,J.J., and Bockstahler,L.E. (2006). Simple and effective method for generating single-stranded DNA targets and probes. Biotechniques *40*, 759-763.

Wan, G., Mathur, R., Hu, X., Liu, Y., Zhang, X., Peng, G., and Lu, X. (2013). Long non-coding RNA ANRIL (CDKN2B-AS) is induced by the ATM-E2F1 signaling pathway. Cell Signal *25*, 1086-1095.